Entropy production of a small quantum system under strong coupling with an environment: A computational experiment

Ketan Goyal [a,1], Xian He [a,b], Ryoichi Kawai [a,*]

[a] *Department of Physics, University of Alabama at Birmingham, Birmingham, AL 35294, USA*
[b] *Department of Physics, Nanchang University, Nanchang 330031, China*

A B S T R A C T

Many theoretical expressions of dissipation along non-equilibrium processes have been proposed. However, they have not been fully verified by experiments. Especially for systems strongly interacting with environments the connection between theoretical quantities and standard thermodynamic observables are not clear. We have developed a computer simulation based on a spin-boson model, which is in principle exact and suitable for testing the proposed theories. We have noted that the dissipation obtained by measuring conventional thermodynamic quantities deviates from the second law of thermodynamics presumably due to the strong coupling. We found that simple correction to entropy makes it more consistent with the second law under the strong coupling regime. This observation appears to be consistent with the theory based on the potential of mean force.

© 2019 Elsevier B.V. All rights reserved.

1. Introduction

The second law of thermodynamics is considered to be one of the most fundamental laws of physics [1]. Yet the precise definition of irreversible entropy production still remains elusive. It is now widely accepted that von Neumann entropy (vN-entropy), $S(\rho) = -\operatorname{tr}\rho\ln\rho$ where ρ is the density operator of the system, represents thermodynamic entropy even in non-equilibrium situations. However, it is invariant under unitary evolution owing to the Liouville theorem and microscopic time reversibility, and thus the entropy of isolated systems never changes. On the other hand, the second law and entropy production can be determined by comparing forward and time-reversed processes [2,3], suggesting that the irreversibility of thermodynamic processes does not conflict with microscopic time reversibility. Esposito–Lindenberg–Van den Broeck has developed a general "non-equilibrium" expression of entropy production based on vN-entropy [4], which is consistent with fluctuation theorems [5]. While the proposed expression is developed under a rather general condition, its validity has not been tested, in particular for systems strongly interacting with environments.

A standard theory of thermodynamics assumes that the interaction energy between a system and environment is negligibly small compared to the system energy. Under such a condition, border lines between a system and environment are obvious and the thermodynamic laws can be expressed only with the state of system. However, the assumption of weak coupling becomes untenable when the system is reduced to a molecular size where the magnitude of the system and coupling energy are of the same order. Then, the separation becomes moot since the interaction energy depends on the state of system and environment simultaneously. Because of this inseparability, standard thermodynamic quantities

---

* Corresponding author.
   E-mail address: kawai@uab.edu (R. Kawai).
[1] Current address: Avigo Solutions, LLC, 1500 District Avenue, Burlington, MA 01803, USA.

such as heat and entropy are no longer clearly defined. It is natural to ask if the thermodynamic laws can be expressed only with the state of the system or if the state of environments must be taken into account. Many works have been reported [4–27] but the issues have not been resolved yet.

In addition to the issue of interaction energy, the correlation between a system and environment, especially quantum entanglement, plays an important role in thermodynamics. For example, the coupling introduces irreversible change in the information entropy through decoherence induced by quantum entanglement between system and environments [28,29]. Moreover, under the strong coupling limit, the system density no longer takes a canonical form [30–32], and is even not diagonal in the energy basis [9,32,33]. It has been suggested that continuous measurement of the system by the environment projects the Gibbs state onto the so-called pointer basis [32]. Continuous measurement also suppresses heat conduction due to the quantum Zeno effect under the strong coupling limit [32,34–36]. Since quantum coherence and entanglement can be used as resources in thermodynamics [26,37–39], the decoherence should be considered as a part of thermodynamic dissipation.

A promising method that takes into account strong coupling was developed long ago by Kirkwood [40], in which an effective Hamiltonian or so-called potential of mean force replaces the Hamiltonian of the system. In this approach, the effects of strong coupling are incorporated into effective thermodynamic quantities such that they satisfy the standard thermodynamics laws. The same idea has recently been extended to stochastic thermodynamics [6,7,9,11,14,16,18,19,27, 33]. In particular, the first and second laws of thermodynamics are redefined with the effective quantities [14,18,27]. In this theory, the laws of thermodynamics with the effective thermodynamic quantities are still determined only by the state of the system. However, the physical meaning of effective thermodynamic quantities and their relation to observable physical quantities are not clear.

The present investigation tries to find where the standard theory of thermodynamics fails due to strong coupling through exact numerical experiments. We observed that the second law is violated if the conventional definition of thermodynamic variables are used. On the other hand, we found that if an appropriate additive correction is applied to entropy and other quantities, the entropy production appears to be consistent with the second law even in the strong coupling regime. In the following, first we introduce a strategy of numerical experiment that determines entropy production from experimentally measurable quantities. Then, a simple model and numerical methods are introduced. Experiments are carried out for various different cases to ensure that the observed results are not specific to a single case. At the end, we will compare the results with the general theories based on Refs. [4,27].

2. Construction of experiments

We first construct a numerical experiment that provides accurate information about the dissipation under a strong coupling regime without evoking non-equilibrium thermodynamics. We measure only well-defined standard thermodynamic quantities. Consider an isolated composite system consisting of a small system S and a large environment B. Initially, they are disconnected. When S is brought into contact with B, certain dissipation takes place. We would like to determine the irreversible entropy produced during the time-dependent interaction between S and B through experimentally measurable quantities only when the system is expected to be in a thermal equilibrium.

The Hamiltonian of the whole system is given by

$$H_{SB} = H_S + H_B + \lambda(t)H_I \tag{1}$$

where H_S and H_B are Hamiltonians for the system and the environment, respectively. The coupling Hamiltonian H_I is switched on and off through a protocol function $1 \geq \lambda(t) \geq 0$. We measure the following energies in the numerical experiment. System energy is simply the mean energy of system:

$$U(t) = \text{tr}_S\{\rho_S(t)H_S\} \tag{2}$$

which should be distinguished from the equilibrium *internal energy* $\mathcal{U}$. Heat is defined as the energy released by the environment,

$$Q(t) = \text{tr}_B\{\rho_B(t_0)H_B\} - \text{tr}_B\{\rho_B(t)H_B\}, \tag{3}$$

and work is the change in total energy

$$W(t) = \text{tr}_{SB}\{\rho_{SB}(t)H_{SB}\} - \text{tr}_{SB}\{\rho_{SB}(t_0)H_{SB}\} \tag{4}$$

where t_0 is initial time. The density operator of the whole system is denoted as ρ_{SB}. The reduced densities $\rho_S = \text{tr}_B \rho_{SB}$ and $\rho_B = \text{tr}_S \rho_{SB}$ represent the state of the system and the environment, respectively. In addition, we measure the coupling energy:

$$V(t) = \lambda(t) \text{tr}_{SB}\left[\rho_{SB}(t)H_I\right]. \tag{5}$$

We assume that the initial state is a product state $\rho_{SB}(t_0) = \rho_S(t_0) \otimes \rho_B^G$ where the environment is in a local Gibbs state $\rho_B^G = e^{-\beta H_B}/\text{tr}_B\left[e^{-\beta H_B}\right]$. The initial system state $\rho_S(t_0)$ is arbitrary. We further assume that $V_I(t_0) = 0$. Our goal is to determine entropy production along non-equilibrium transformation between the uncoupled state ($\lambda = 0$) and the fully

coupled state ($\lambda = 1$). Based on the standard theory of thermodynamics, internal energy $\mathcal{U}$, entropy $\mathcal{S}$ and free energy $\mathcal{F}$ are only well defined at thermal equilibrium. There are two ways to determine the entropy production, one from heat and the other from work,

$$\Sigma^{\mathrm{Q}} = \Delta\mathcal{S} - \beta Q \tag{6}$$

$$\Sigma^{\mathrm{W}} = \beta\left(W - \Delta\mathcal{F}\right) \tag{7}$$

where free energy difference is defined by $\Delta\mathcal{F} = \mathcal{F}(\lambda = 1) - \mathcal{F}(\lambda = 0)$ and entropy difference by $\Delta\mathcal{S} = \mathcal{S}(\lambda = 1) - \mathcal{S}(\lambda = 0)$. Strictly speaking, these two expressions of entropy production are valid only for a transition between two equilibrium states and should take the same value. We assume that the definitions of dissipation (3) and (4) are valid even when the coupling is strong. Similar mathematical expressions for the entropy production between non-equilibrium states have been proposed as discussed below. However, the present numerical experiment determines the entropy production solely based on Eqs. (3) and (4).

First, we try to find information about equilibrium states, namely $\Delta\mathcal{F}$ and $\Delta\mathcal{S}$. Since the initial state is not at an equilibrium, we must relax it by connecting the system to the environment. For this purpose, we consider a "quasi-static" protocol (protocol 1):

$$\lambda_1(t) = \begin{cases} \text{slowly turn on coupling} & t_1 > t > t_0 \\ \text{keep coupling constant} & t_2 > t > t_1 \\ \text{slowly turn off coupling} & t_3 > t > t_2 \\ \text{keep coupling off} & t_4 > t > t_3 \end{cases} \tag{8}$$

Each step takes a sufficiently long time that the process is quasi-static. However, since the initial state of the system is not necessarily at thermal equilibrium, the whole process is also not necessarily reversible. During the first period, the initial non-equilibrium state relaxes to an equilibrium, and irreversible dissipation completes before t_1. No further dissipation takes place after t_1. Then, we measure heat and work at t_2 and t_4 when the system is guaranteed to be in thermodynamic equilibrium. Under the strong coupling regime, we do not know the equilibrium state at $\lambda = 1$ and thus these measurements are necessary.[2]

Since protocol 1 is quasi-static and the Hamiltonian returns to the starting point, any heat during the whole process is entirely dissipative and the corresponding entropy production

$$\Sigma_1^{\mathrm{Q}}(t_4) = -\beta Q_1(t_4) \tag{9}$$

is entirely due to the relaxation of the initial non-equilibrium state, where $Q_1(t)$ is the net heat along protocol 1 (thermodynamic quantities with index 1 are measured along protocol 1). From the first law, the corresponding dissipative work is $W_1(t_4) + \Delta U$ where $\Delta U = U(t_0) - U(t_4)$ is the energy difference between the initial state and thermal equilibrium at $\lambda = 0$. The dissipation obtained from work is

$$\Sigma_1^{\mathrm{W}}(t_4) = \beta\left[W_1(t_4) + \Delta U\right]. \tag{10}$$

Next we determine $\Delta\mathcal{F}$ and $\Delta\mathcal{S}$. Noting that the system has reached a new equilibrium ($\lambda = 1$) by t_2 and no dissipation takes place afterward, the free energy and entropy differences between the fully detached and connected states are determined as

$$\Delta\mathcal{S} = \beta\left[Q_1(t_2) - Q_1(t_4)\right] \tag{11}$$

$$\Delta\mathcal{F} = W_1(t_2) - W_1(t_4). \tag{12}$$

Once we have determined $\Delta\mathcal{S}$ and $\Delta\mathcal{F}$, we can determine the dissipation from the measurement at t_2. Combining Eqs. (9) and (11), and also Eqs. (10) and (12), we obtain

$$\Sigma_1^{\mathrm{Q}}(t_2) = \Delta\mathcal{S} - \beta Q_1(t_2) \tag{13}$$

$$\Sigma_1^{\mathrm{W}}(t_2) = W_1(t_2) - \Delta\mathcal{F} + \Delta U. \tag{14}$$

Despite that the system is initially not at thermal equilibrium, Eq. (13) suggests that the standard thermodynamic expression (6) is still valid. On the other hand, Eq. (14) differs from (7) by ΔU. Based on this we define non-equilibrium free energy change as $\Delta F = \Delta\mathcal{F} - \Delta U$.

Now we turn to non-equilibrium processes. As an extreme case, we turn on the coupling instantaneously. In protocol 2, $\lambda_2(t)$ remains zero during the first period ($t_1 > t > t_0$) but it is identical to protocol 1 for the remaining periods. Since $V_I = 0$, no work is done by the sudden change of λ. The process after t_1 is quasi-static, but the system relaxes to an equilibrium ($\lambda = 1$) between t_1 and t_2, during which dissipation takes place. Similarly to protocol 1, the net heat is entirely dissipative and thus the net entropy production for the second protocol is given by

$$\Sigma_2^{\mathrm{Q}}(t_4) = -\beta Q_2(t_4) \tag{15}$$

---

[2] In real experiments, the two measurements must be done in separate experiments since the measurement at t_2 changes the quantum states afterward.
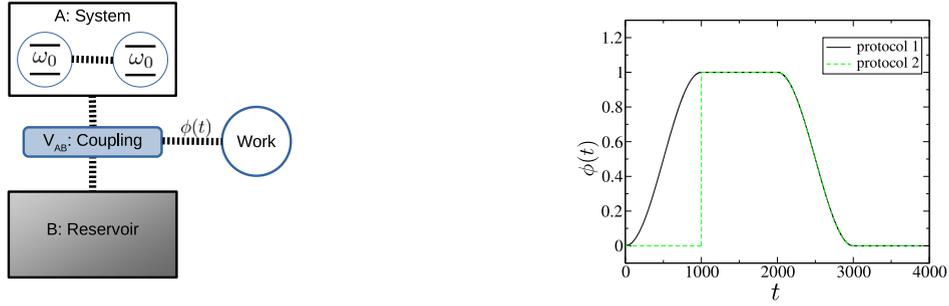
(a) A pair of qubits in a system S is connected to and disconnected from an environment through the time-dependent protocol $\lambda(t)$. During transition periods, work is done through the time-varying coupling.

(b) Two protocols. The coupling is turned on slowly in protocol 1 and instantaneously in protocol 2. In both protocols, the coupling is slowly turned off.

Fig. 1. Model.

$$\Sigma_2^W(t_4) = \beta\left[W_2(t_4) + \Delta U\right] \tag{16}$$

where ΔU is already measured with the protocol 1.

Since the process after t_2 is reversible,

$$\Delta\mathcal{S} = \beta\left[Q_2(t_2) - Q_2(t_4)\right] \tag{17}$$

$$\Delta\mathcal{F} = W_2(t_2) - W_2(t_4). \tag{18}$$

Combining Eq. (15) with (17) and Eqs. (16) with (18), we obtain

$$\Sigma_2^Q(t_2) = \Delta\mathcal{S} - \beta Q_2(t_2) = \beta\left[Q_1(t_2) - Q_1(t_4) - Q_2(t_2)\right] \tag{19}$$

$$\Sigma_2^W(t_2) = W_2(t_2) - \Delta\mathcal{F} + \Delta U = \beta\left[W_2(t_2) - W_1(t_2) + W_1(t_4) - \Delta U\right]. \tag{20}$$

where we used Eqs. (11) and (12) for $\Delta\mathcal{S}$ and $\Delta\mathcal{F}$ instead of Eqs. (17) and (18).

We have used only the standard theory of thermodynamics based on the transition between equilibrium states and thus the dissipation measured at t_2 and t_4 are considered correct. Some measurements are redundant but they serve as a benchmark test of the computational experiment. Any proposed theory of dissipation as a function of time must pass through these well established values.

Now, we try to extend the expression of dissipation to a "non-equilibrium" expression (time-dependent expression) for the period where dissipation is actually taking place ($t_2 > t > t_1$). Since no work is done during this period, time-dependent dissipation based on work is not possible. Therefore, we determine the dissipation from heat. By direct comparison between Eqs. (9) and (19), we note that difference is $Q_1(t_2) - Q_2(t_2)$. As a possible candidate of a non-equilibrium expression, we just replace t_2 with t:

$$\Sigma^Q(t) = \beta\left[Q_1(t) - Q_2(t) - Q_1(t_4)\right], \qquad t > t_1. \tag{21}$$

which takes the correct values at the two equilibrium measurement points t_2 and t_4. However, its validity is not certain for $t_2 > t > t_1$.

Esposito et al. [4] has proposed a promising expression:

$$\Sigma^S(t) = \Delta S_s(t) - \beta Q(t) \tag{22}$$

which is strictly positive. It replaces the reversible entropy change $\beta\left[Q_1(t) - Q_1(t_4)\right]$ in Eq. (21) with the change in vN-entropy $\Delta S_s(t) = -\operatorname{tr}_s \rho_s(t) a \ln \rho_s(t) + \operatorname{tr}_s \rho_s(t_0) \ln \rho_s(t_0)$. One important feature of this expression is that the dissipation due to decoherence is explicitly included. It has also been claimed that this expression is valid even when the coupling is strong. However, this is not obvious from the thermodynamics point of view.

In the next section, we construct a simple model and measure the *conventional* entropy production from expressions (15)–(19), which serves as a benchmark for the proposed theory. The two *non-equilibrium* expressions of entropy production (21) and (22) are evaluated, and their validity will be checked.

3. Model

We consider a simple spin-boson model in which a pair of coupled qubits interact with an environment consisting of an ideal Bose gas. (See Fig. 1a.) The Hamiltonian of the system is given by

$$H_s = \frac{\omega_0}{2}\sigma_z \otimes I + \frac{\omega_0}{2}I \otimes \sigma_z + \Lambda(\sigma_+ \otimes \sigma_- + \sigma_- \otimes \sigma_+) \tag{23}$$

where ω_0 and Λ are the excitation energy of the individual qubits and the coupling strength between them, respectively. We use $\omega_0 = 1$ and $\Lambda = 0.5$ for all case studies. (All energies are scaled with ω_0 throughout the paper.)

The environment is an infinitely large ideal Bose gas with Hamiltonian

$$H_{\mathrm{B}} = \sum_{j \geq 1} \omega_j a_j^\dagger a_j \tag{24}$$

and interacts with the system through a bilinear form of coupling Hamiltonian

$$H_{\mathrm{I}}(t) = \lambda(t) X_{\mathrm{S}} \otimes Y_{\mathrm{B}} \tag{25}$$

where the strength of the coupling is controlled by a protocol $0 \leq \lambda(t) \leq 1$. The environment side of the bilinear coupling is a displacement of the environment

$$Y_{\mathrm{B}} = \sum_j v_j \left(a_j^\dagger + a_j \right). \tag{26}$$

with coupling strength v_j between the system and jth mode. The spectral density of the environment is assumed to be of the Drude–Lorentz type

$$J(\omega) = \frac{2g}{\pi} \frac{\omega \gamma}{\omega^2 + \gamma^2} \tag{27}$$

where g and γ are the coupling strength and relaxation rate, which are fixed at $g = 1$ and $\gamma = 0.1$ in the present investigation. For the system side of the bilinear coupling, we will explore various different X_{S}.

We assume that the whole system is completely isolated and its unitary evolution is determined by the Liouville–von Neumann equation, $\frac{d}{dt} \rho_{\mathrm{SB}} = -i[H_{\mathrm{SB}}, \rho_{\mathrm{SB}}]$. Taking its partial trace, the reduced density follows a non-unitary evolution

$$\frac{d}{dt} \rho_{\mathrm{S}} = -i[H_{\mathrm{S}}, \rho_{\mathrm{S}}] - i\lambda(t)[X_{\mathrm{S}}, \eta_{\mathrm{S}}] \tag{28}$$

where $\eta_{\mathrm{S}} = \mathrm{tr}_{\mathrm{B}} (Y_{\mathrm{B}} \rho_{\mathrm{SB}})$ is an operator in the system Hilbert space. If the initial state is a product state $\rho_{\mathrm{SB}}(t_0) = \rho_{\mathrm{S}}(t_0) \otimes \rho_{\mathrm{B}}^{\mathrm{G}}$, then Eq (28) can be numerically solved using the method of hierarchical equations of motion (HEOM) [34,41] and the results are in principle exact and limited only by numerical implementation. A brief summary of HEOM is given in Appendix. The operator η_{S} contains sufficient information about the state of the environment and allows us to evaluate various thermodynamic quantities.

Heat (3), work (4), and coupling energy (5) are computed as

$$Q = -\int_{t_0}^t \left(\mathrm{tr}_{\mathrm{S}} [H_{\mathrm{S}} \dot{\rho}_{\mathrm{S}}(\tau)] + \lambda(\tau) \mathrm{tr}_{\mathrm{S}} [X_{\mathrm{S}} \dot{\eta}(\tau)] \right) d\tau , \tag{29}$$

$$W = \int_{t_0}^t \dot{\lambda}(\tau) \mathrm{tr}_{\mathrm{S}} \{X_{\mathrm{S}} \eta(\tau)\} d\tau , \tag{30}$$

and

$$V = \lambda(t) \mathrm{tr}_{\mathrm{S}} \{X_{\mathrm{S}} \eta_{\mathrm{S}}(t)\} , \tag{31}$$

which satisfy the conservation of energy $W + Q = \Delta U + \Delta V$. In addition, we monitor the presence of system–environment correlation by computing the correlation function

$$C_{\mathrm{SB}}(t) \equiv \langle X_{\mathrm{S}} \otimes Y_{\mathrm{B}} \rangle - \langle X_{\mathrm{S}} \rangle \langle Y_{\mathrm{B}} \rangle = \mathrm{tr}_{\mathrm{S}} (X_{\mathrm{S}} \eta_{\mathrm{S}}) - \mathrm{tr}_{\mathrm{S}} (X_{\mathrm{S}} \rho_{\mathrm{S}}) \cdot \mathrm{tr}_{\mathrm{S}} (\eta_{\mathrm{S}}) . \tag{32}$$

The quasi-static process is emulated by protocol 1:

$$\lambda_1(t) = \begin{cases} \sin^2 \left[\dfrac{\pi t}{2\tau} \right] & \tau > t > 0 \\ 1 & 2\tau > t > \tau \\ \sin^2 \left[\dfrac{\pi(3\tau - t)}{2\tau} \right] & 3\tau > t > 2\tau \\ 0 & 4\tau > t > 3\tau \end{cases} \tag{33}$$

where we define $t_n = n\tau$. In the present work, we fix $\tau = 1000$. (See Fig. 1b.) For the relaxation experiment (protocol 2), $\lambda_2(t) = 0$ for $\tau > t > 0$ and otherwise $\lambda_2(t) = \lambda_1(t)$. This allows us to compare equilibrium and non-equilibrium states easily on the plots.
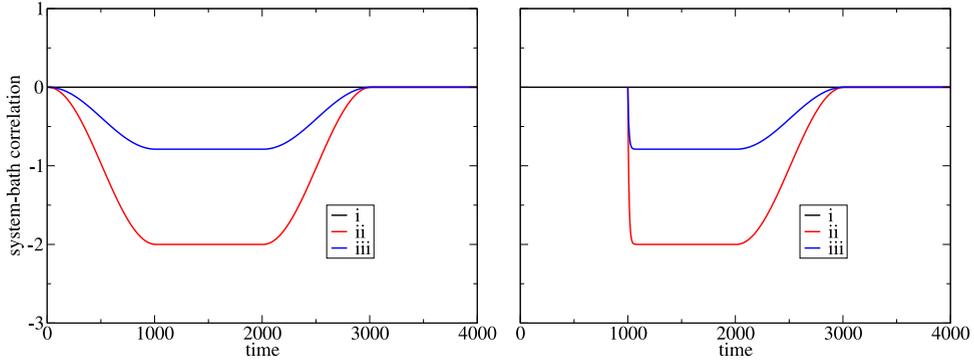
Fig. 2. Correlation between system and environment for the three initial states given in Eq (34) during protocol 1 (left) and protocol 2 (right). Initial state (i) shows no correlation at all. Other initial states, (ii) and (iii) form quantum and classical correlation, respectively. The formation of correlation is rather quick as shown in the right panel.

4. Case studies

We choose three particular initial states:

$$\rho_s(t_0) = \begin{cases} \text{(i)} & |00\rangle\langle00| \\ \text{(ii)} & \dfrac{1}{2}\left(|00\rangle\langle00| + |00\rangle\langle11| + |11\rangle\langle00| + |11\rangle\langle11|\right) \\ \text{(iii)} & e^{-\beta H_s}/\text{tr}\left(e^{-\beta H_s}\right) \end{cases} \tag{34}$$

which allow us to control system–environment correlation.

In the present investigation, we mainly consider a special choice of coupling $X_s = H_s$. Since H_s commutes with the total Hamiltonian, the energy of the system conserves, i.e., $\Delta U = 0$. In other words, heat released by the environment never enters the system but it stored in the coupling, which signifies the effect of coupling energy in thermodynamic processes. Moreover, the diagonal elements of the reduced density ρ_s in the energy basis are invariant. Hence the system entropy changes only through the decoherence. We also consider another form of coupling, $X_s = \sigma_x \otimes I + I \otimes \sigma_x$.

4.1. Case I

Initial state (i) is an energy eigenstate, which is protected from the environment by $X_s = H_s$. Since the system remains in the same pure state, no correlation of any kind is formed throughout the time evolution. Fig. 2 confirms that there is no system–environment correlation and thus the whole system remains in a product state. Entropy production takes place only in the environment. Fig. 3a plots the energy changes. For protocol 1, both work and heat vanish at the end, certifying that the process is quasi-static. For protocol 2, both work and heat reach the same value at t_4. Using Eqs. (9) and (10), we find $\Sigma^Q(t_4) = \Sigma^W(t_4) = 1.0$, which is the dissipation incurred during initial relaxation. At the other checkpoint t_2, we obtain entropy production $\Sigma^Q(t_2) = \Sigma^W(t_2) = 0.98$ from Eqs. (19) and (20). The slight difference between the two checkpoints is due to the small dissipation caused by the finite time protocols. Based on these observations, we conclude that the simulation produces a standard thermodynamic behavior of the quasi-static and relaxation processes.

Next, we plot non-equilibrium expressions (21) and (22) in Fig. 3b. After the rapid relaxation period, Σ^Q reaches the correct dissipation and passes through the two checkpoints. On the other hand, Σ^s shows disagreement. While the correct value is reached at the end, it grossly overestimates the dissipation at the checkpoint t_2. As mathematically proven, Σ^S is always positive, consistent with the second law, but its derivative is clearly negative between t_2 and t_3. Hence, Σ^s cannot be considered a valid definition of entropy production. Zooming into the period where the dissipation actually takes place (the bottom panel of Fig. 3b), Σ^Q initially goes down below 0, which is incompatible with the second law. We found that neither Σ^Q nor Σ^s is consistent with the second law.

However, we have noticed that if the entropy is redefined as $S(t) \rightarrow S(t) + \frac{1}{2}V(t)$, both Σ^Q and Σ^s coincide and become consistent with the second law. Based on these observations, we introduce two empirical expressions of entropy production:

$$\Sigma^{QV}(t) = \Sigma^Q(t) + \frac{1}{2}\left[V_1(t) - V_2(t)\right] \tag{35}$$

and

$$\Sigma^{SV}(t) = \Sigma^s(t) + \frac{1}{2}V_2(t) \tag{36}$$

where $V_1(t)$ and $V_2(t)$ are the coupling energy along protocol 1 and 2, respectively. Fig. 3b shows that Σ^{QV} and Σ^{SV} both monotonically increase to the correct value as expected from the second law.
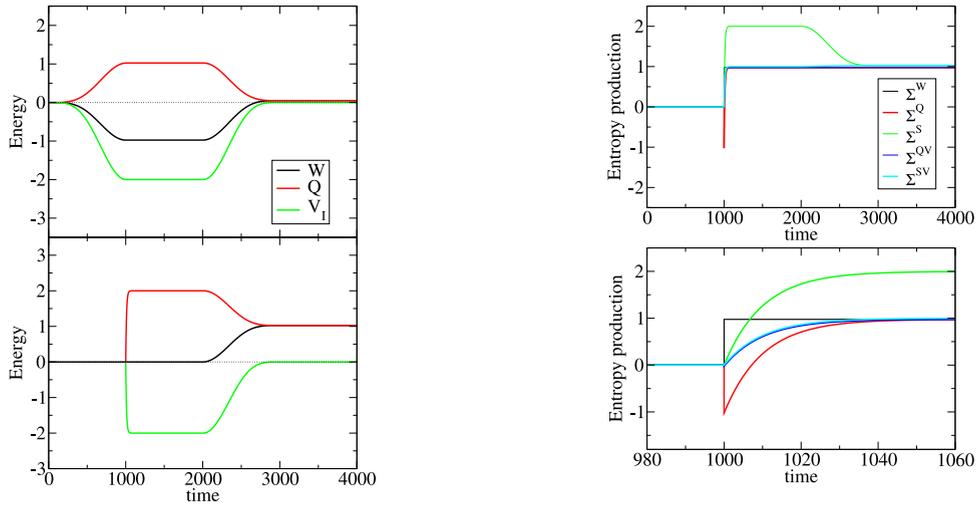
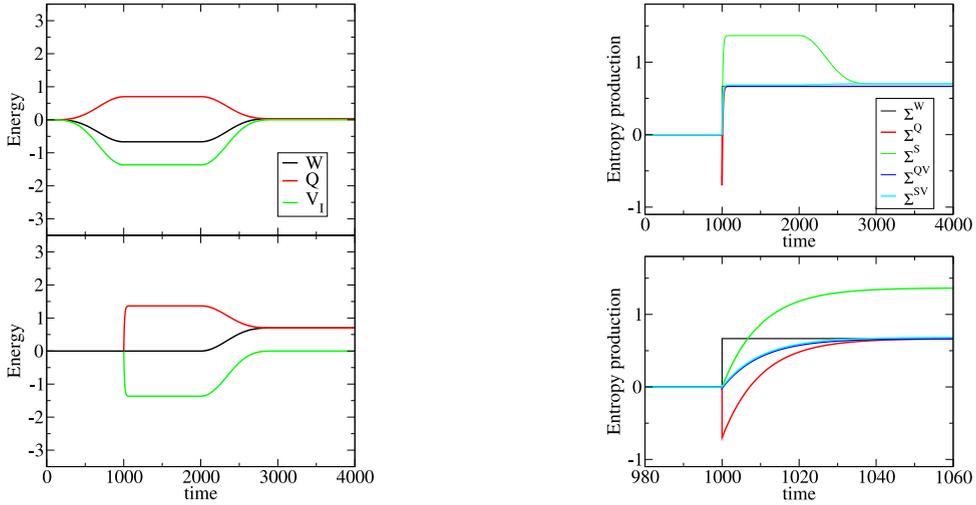(a) Energy transaction during protocol 1 (top) and 2 (bottom).

(b) Various definitions of entropy production evaluated from the computer experiment. The top panel shows the whole process and the bottom magnifies the period where the relaxation process takes place.

Fig. 3. Time evolution of various thermodynamic quantities for case I.
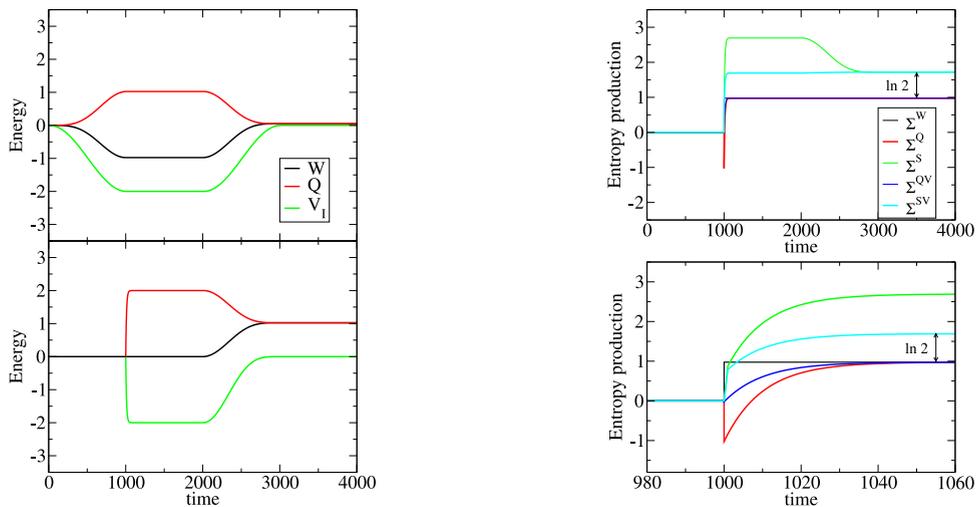
(a) Energy transaction during protocol 1 (top) and 2 (bottom).

(b) Various definitions of entropy production evaluated from the computer experiment. The top panel shows the whole process and the bottom magnifies the period where the relaxation process takes place.

Fig. 4. Time evolution of various thermodynamic quantities for case II.

4.2. Case II

The coupling operator X_s is still H_s. Initial state (ii) is a superposition of two energy eigenstates, which is subject to decoherence due to quantum entanglement with the environment. The off-diagonal elements of the initial pure state vanish and S_s increases.

Fig. 2 indeed shows a strong system–environment correlation, which is presumably due to entanglement. In terms of energy transaction, this case is almost identical to case I, and the thermodynamic dissipation measured at two checkpoints

(a) Energy transaction during protocol 1 (top) and 2 (bottom).

(b) Various definitions of entropy production evaluated from the computer experiment. The top panel shows the whole process and the bottom magnifies the period where the relaxation process takes place.

Fig. 5. Time evolution of various thermodynamic quantities for case III.

are consistent (Fig. 4a). The entropy production evaluated from heat, Σ^{Q} failed in the same way as in the previous case. Similarly, Σ^{s} failed as well. Applying the same empirical correction introduced in case I, Σ^{QV} monotonically increases to the value obtained from $\Sigma^{W}(t_4)$ and $\Sigma^{Q}(t_4)$. Hence, it is consistent with thermodynamics. On the other hand, Σ^{sv} reaches a higher value due to the decoherence-induced entropy production. When the decoherence is perfect, $\ln 2$ of irreversible entropy is expected. Fig. 4b shows that $\Sigma^{sv} - \Sigma^{QV} = \ln 2$, in good agreement.

4.3. Case III

We still keep the same X_s. The system starts with a Gibbs state (iii) with the same temperature as the environment and thus the whole system is in thermal equilibrium at the beginning. It is a classical mixture of the energy eigenstates protected from the environment, thus only the classical correlation between the system and environment can be formed, and the S_s remains constant. Fig. 2 shows a weaker correlation than the entanglement in case II. Since the initial state is diagonal, there is no decoherence and thus Σ^{QV} and Σ^{sv} are nearly identical. Both Σ^{Q} and Σ^{s} fail as in the previous cases, and the empirical expressions work for this case as well (see Fig. 5).

4.4. Case IV

We consider a more realistic coupling $X_s = \sigma_x \otimes I + I \otimes \sigma_x$. Due to the symmetry between the two qubits, the singlet state (decoherence-free state) is protected from the environment. The remaining triplet states are thermalized. Unlike the previous special cases, the system energy relaxes and thus some portion of heat flows into the system. Starting with the non-equilibrium initial state (ii), we expect that both classical and quantum correlations are formed. The energy transactions plotted in Fig. 6a are a little more complicated than the previous cases. Fig. 6b shows that Σ^{Q} and Σ^{s} fail in the same way as before. Remarkably, both Σ^{QV} and Σ^{sv} still behave reasonably and seem consistent with the second law despite energy exchanges between the system and the environment. The dissipation due to decoherence is clearly visible in $\Sigma^{sv} - \Sigma^{QV}$.

5. Discussion

We found that the entropy production Σ^{S} proposed in Ref. [4] is not consistent with the second law as it is. The conventional interpretation of dissipation defined by Eq. (21) also failed. However, the empirical redefinition of entropy (35) and (36) made them more consistent. In order to justify the correction, we briefly review the more recent theory based on the potential of mean force [6,7,9,14,18,19,27,33]. Here we use the quantum version based on Ref. [27].
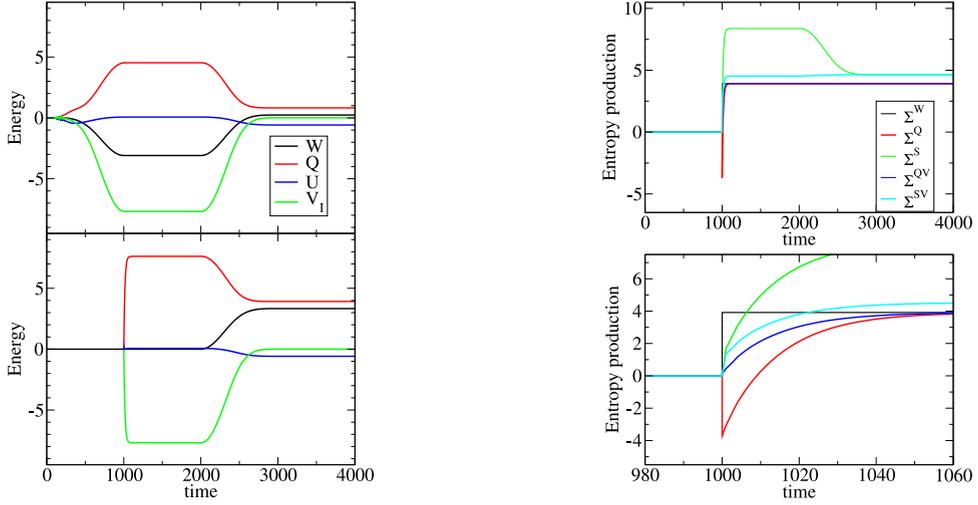
(a) Energy transaction during protocol 1 (top) and 2 (bottom).

(b) Various definitions of entropy production evaluated from the computer experiment. Whole process (top) and during the relaxation process takes place (bottom).

Fig. 6. Time evolution of various thermodynamics quantities for case IV.

First the theory assumes that the whole system is in a canonical equilibrium and defines a temperature β for a given energy by

$$E_{\text{total}} = \text{tr}_{\text{SB}} \left\{ (H_{\text{S}} + H_{\text{B}} + V_{\text{SB}}) e^{-\beta(H_{\text{S}} + H_{\text{B}} + V_{\text{SB}})} \right\} / Z_{\text{SB}} \tag{37}$$

where $Z_{\text{SB}} = \text{tr}_{\text{SB}} \left\{ e^{-\beta(H_{\text{S}} + H_{\text{B}} + V_{\text{SB}})} \right\}$. Assuming that the reference temperature does not change over time, an effective Hamiltonian [27] for the system is defined by

$$\tilde{H}_{\text{S}} = -\frac{1}{\beta} \ln \left[\text{tr}_{\text{B}} \left\{ e^{-\beta(H_{\text{S}} + H_{\text{B}} + V_{\text{SB}})} \right\} / Z_{\text{B}} \right] \tag{38}$$

with $Z_{\text{B}} = \text{tr}_{\text{B}} \, e^{-\beta H_{\text{B}}}$. Further, the effective thermodynamic quantities are redefined for an arbitrary state of the system $\rho_{\text{S}}(t)$ by

$$\tilde{U} = U + \tilde{U}' + \tilde{U}'' \tag{39}$$

$$\tilde{S} = S_{\text{s}} + \beta \tilde{U}'' \tag{40}$$

$$\tilde{F} = F + \tilde{U}' \tag{41}$$

$$\tilde{Q} = Q - \Delta V_{\text{SB}} + \tilde{U}' + \Delta \tilde{U}'' \tag{42}$$

where the additive correction terms are defined by

$$\tilde{U}' = \text{tr}_{\text{s}} \{ \rho_{\text{s}}(t)(\tilde{H}_{\text{s}} - H_{\text{s}}) \} \tag{43a}$$

$$\tilde{U}'' = \text{tr}_{\text{s}} \{ \rho_{\text{s}}(t) \tilde{\beta} \partial_{\beta} \tilde{H}_{\text{s}} \}. \tag{43b}$$

These effective quantities satisfy usual thermodynamic relations. Using these definitions along with the first law $W + \tilde{Q} = \Delta \tilde{U}$ we find an expression of entropy production

$$\tilde{\Sigma} = \Sigma^{\text{s}} + \beta \tilde{U}' \tag{44}$$

The present empirical correction is equivalent to $\tilde{U}' = \tilde{U}'' = \frac{1}{2}V_I$. Then, the effective thermodynamic quantities become

$$\tilde{U} = U + V_I \tag{45a}$$

$$\tilde{S} = S_s + \frac{1}{2}V_I \tag{45b}$$

$$\tilde{F} = F + \frac{1}{2}V_I \tag{45c}$$

$$\tilde{Q} = Q \tag{45d}$$

$$\tilde{\Sigma} = \Sigma^s + \frac{1}{2}V_I. \tag{45e}$$

Admittedly we are not able to derive the correction terms from first principles. We do not claim that they are exact. However, the correction obtained from the potential of mean force is quite consistent with our finding. On the other hand, the correction terms in the mean force theory do not depend on the state of environment whereas the coupling energy does. So, the correspondence between the mean force theory and our results is still not clear. Further theoretical investigation is needed.

6. Conclusion

We have developed an exact numerical experiment of qubits strongly coupled to a thermal environment. Information about equilibrium states is obtained from a slow protocol mimicking a quasi-static process. The dissipation during relaxation processes is measured based on standard thermodynamic principles. Based on the entropy production obtained from the experiment and the standard relation between entropy and heat, we defined a time-dependent expression of entropy production consistent with the observed value. Then, we tested it along with a theoretical expression. Neither was found to be consistent with the second law. However, a simple additive correction to entropy makes them consistent with the second law. For the current model, the correction is one half the coupling energy. Accordingly, other quantities need to be adjusted to satisfy the 1st and 2nd laws. The results are qualitatively consistent with the theory based on the potential of mean force.

Acknowledgments

Appendix. Hierarchical equations of motion

In 1990, Tanimura [41] showed that the Feynman–Vernon influence functional can be obtained from an infinite set of ordinary differential equations called hierarchical equations of motion (HEOM). It does not invoke any approximation, and its accuracy is solely determined by its numerical implementation. Therefore, the results are in principle exact and non-Markovian effects, essential to the strongly coupled regime, are fully taken into account. Since HEOM has been already used to study open quantum systems by other groups, we only briefly describe the method. More details can be found in Ref. [42]

When the environments are ideal Bose gases, the influence functional can be written in a super-operator form $e^{i\Phi(t,t_0)}$ where the super-operator is given in the interaction picture by [43,44]

$$i\Phi(t, t_0) = \int_{t_0}^{t} ds \int_{t_0}^{s} ds' \, \lambda(s)\lambda(s') \mathcal{S}^-(s) \left\{ i\kappa_i(s - s')\mathcal{S}^-(s') - \kappa_r(s - s')\mathcal{S}^+(s') \right\} \tag{A.1}$$

where we introduce super-operators $\mathcal{S}^\pm = [X_s, \cdot]_\mp$. The dissipation kernel κ_r and noise kernel κ_i are

$$\kappa_i(\tau) = \sum_j \frac{\nu_j^2}{2m_j\omega_j} \sin \omega_j\tau \qquad \kappa_r(\tau) = \sum_j \frac{\nu_j^2}{2m_j\omega_j} \coth \left(\frac{\omega_j\beta}{2} \right) \cos \omega_j\tau \tag{A.2}$$

where m_j and ω_j are mass and frequency of the jth harmonic oscillator. The coupling strength ν_j is defined in Eq. (26). When the Drude–Lorentz spectrum (27) is used, the kernels decay multi-exponentially [45]. At a relatively high temperature, which we assumed for the environments, the kernels can be expressed as

$$\kappa_r(\tau) - i\kappa_i(\tau) = \lambda \left(c_1 e^{-\gamma_1 \tau} + c_2 e^{-\gamma_2 \tau} + 2c_0\delta(\tau) \right). \tag{A.3}$$

The constants c_j and γ_j can be obtained by various fitting methods. We used the values given in [46].

Using the influence functional, the system density operator at t can be written as $\rho_s(t) = e^{i\Phi(t,t_0)}\rho_s(t_0)$. However, applying the super-operator on the initial density is still a major difficulty in the influence functional approach. HEOM avoids the difficulty of the exponential super-operator. By differentiating $\rho_s(t)$ with respect to time t, we find

$$\frac{d}{dt}\rho_s(t) = -gc_0\lambda^2(t)\mathcal{S}^-(t)\mathcal{S}^-(t)\rho_s(t) - ig\lambda(t)\mathcal{S}^-(t)\left[\zeta_{1,0}(t) + \zeta_{0,1}(t)\right] \tag{A.4}$$

where we introduced two auxiliary operators

$$\zeta_{1,0}(t) = -i\left(\int_{t_0}^t ds\,\lambda(s)e^{-\gamma_1(t-s)}\mathcal{G}_1(s)\right)$$
$$\times \prod_j \exp\left[-g\int_{t_0}^t ds_1 \int_{t_0}^{s_1} ds_2\,\lambda(s_1)\lambda(s_2)\mathcal{S}^-(s_1)e^{-\gamma_j(s_1-s_2)}\mathcal{G}_j(s_2)\right]\rho_s(0) \tag{A.5}$$

$$\zeta_{0,1}(t) = -i\left(\int_{t_0}^t ds\,\lambda(s)e^{-\gamma_2(t-s)}\mathcal{G}_2(s)\right)$$
$$\times \prod_j \exp\left[-g\int_{t_0}^t ds_1 \int_{t_0}^{s_1} ds_2\,\lambda(s_1)\lambda(s_2)\mathcal{S}^-(s_1)e^{-\gamma_j(s_1-s_2)}\mathcal{G}_j(s_2)\right]\rho_s(0) \tag{A.6}$$

and another super operator

$$\mathcal{G}_j(t) = \text{Re}\{c_j\}\mathcal{S}^-(t) + i\,\text{Im}\{c_j\}\mathcal{S}^+(t) \tag{A.7}$$

In order to find $\zeta_{0,1}$ and $\zeta_{1,0}$, we differentiate Eqs. (A.5) and (A.6) which leads to a new set of auxiliary operators. By repeating the differentiation, we obtain a hierarchy of differential equations (now in the Schroödinger picture):

$$\frac{d}{dt}\zeta_{n_1,n_2}(t) = -i\left[H_s, \zeta_{n1,n2}(t)\right]_-$$
$$- (\gamma_1 n_1 + \gamma_2 n_2)\zeta_{n1,n2}(t) - g\,c_0\,\lambda^2(t)\mathcal{S}^-\mathcal{S}^-\,\zeta_{n1,n2}(t)$$
$$- in_1\lambda(t)\mathcal{G}_1\,\zeta_{n_1-1,n_2}(t) - in_2\lambda(t)\mathcal{G}_2\,\zeta_{n_1,n_2-1}(t)$$
$$- ig\,\lambda(t)\mathcal{S}^-\left\{\zeta_{n_1+1,n_2}(t) + \zeta_{n1,n2+1}(t)\right\}. \tag{A.8}$$

Since the super-operators $S^\pm$ directly act on the Liouville space, we can evaluate the right hand side of Eq. (A.8) without any difficulty. Now the problem of exponential super-operator is replaced with an infinite set of ODEs. The system density is at the top of the hierarchy $\rho_s(t) = \zeta_{0,0}(t)$ and the moment operator $\eta_s(t)$ is obtained from the auxiliary operators as

$$\eta_s(t) = \lambda(t)\left[\zeta_{1,0}(t) + \zeta_{0,1}(t) + ic_0\mathcal{S}^-\zeta_{0,0}(t)\right]. \tag{A.9}$$

Going down the hierarchy the contribution of deeper levels to the top three auxiliary operators becomes negligible and the hierarchy can be terminated at a certain depth without losing the accuracy of ρ_s and η_s. The acceptable cutoff depth depends on the coupling strength. For a system strongly coupled with environments, we must include many auxiliary operators of deeper depth. In the present simulation, the depth $d = 50 \sim 70$ is found to be enough.

References

[1] A.S. Eddington, The Nature of the Physical World, The Macmillian Company, New York, 1927.
[2] R. Kawai, J.M.R. Parrondo, C. Van den Broeck, Dissipation: The phase-space perspective, Phys. Rev. Lett. 98 (2007) 080602, http://dx.doi.org/10.1103/PhysRevLett.98.080602.
[3] J.M.R. Parrondo, C.V. den Broeck, R. Kawai, Entropy production and the arrow of time, New J. Phys. 11 (7) (2009) 073008, http://dx.doi.org/10.1088/1367-2630/11/7/073008.
[4] M. Esposito, K. Lindenberg, C. Van den Broeck, Entropy production as correlation between system and reservoir, New J. Phys. 12 (2010) 013013.
[5] K. Funo, M. Ueda, T. Sagawa, Quantum fluctuation theorems, in: F. Binder, L. Correa, C. Gogolin, J. Anders, G. Adesso (Eds.), Thermodynamics in the Quantum Regime, Springer, 2019, pp. 249–273, http://dx.doi.org/10.1007/978-3-319-99046-0_10.
[6] M.F. Gelin, M. Thoss, Thermodynamics of a subensemble of a canonical ensemble, Phys. Rev. E 79 (2009) 051121, http://dx.doi.org/10.1103/PhysRevE.79.051121.
[7] M. Campisi, D. Zueco, P. Talkner, Thermodynamic anomalies in open quantum systems: Strong coupling effects in the isotropic xy model, Chem. Phys. 375 (2) (2010) 187–194, http://dx.doi.org/10.1016/j.chemphys.2010.04.026.
[8] I. Kim, G. Mahler, Clausius inequality beyond the weak-coupling limit: The quantum brownian oscillator, Phys. Rev. E 81 (2010) 011101, http://dx.doi.org/10.1103/PhysRevE.81.011101.
[9] S. Hilt, B. Thomas, E. Lutz, Hamiltonian of mean force for damped quantum systems, Phys. Rev. E 84 (2011) 031110, http://dx.doi.org/10.1103/PhysRevE.84.031110.
[10] R. Gallego, A. Riera, J. Eisert, Thermal machines beyond the weak coupling regime, New J. Phys. 16 (12) (2014) 125009, http://dx.doi.org/10.1088/1367-2630/16/12/125009.
[11] M. Esposito, M.A. Ochoa, M. Galperin, Nature of heat in strongly coupled open quantum systems, Phys. Rev. B 92 (23) (2015) 235440, http://dx.doi.org/10.1103/PhysRevB.92.235440.
[12] C. Wang, J. Ren, J. Cao, Nonequilibrium energy transfer at nanoscale: A unified theory from weak to strong coupling, Sci. Rep. 5 (2015) 11787, http://dx.doi.org/10.1038/srep11787.

[13] D. Gelbwaser-Klimovsky, A. Aspuru-Guzik, Strongly coupled quantum heat machines, J. Phys. Chem. Lett. 6 (17) (2015) 3477–3482, http://dx.doi.org/10.1021/acs.jpclett.5b01404.
[14] U. Seifert, First and second law of thermodynamics at strong coupling, Phys. Rev. Lett. 116 (2016) 020601, http://dx.doi.org/10.1103/PhysRevLett.116.020601.
[15] G. Katz, R. Kosloff, Quantum thermodynamics in strong coupling: Heat transport and refrigeration, Entropy 18 (5) (2016) http://dx.doi.org/10.3390/e18050186.
[16] R. Uzdin, A. Levy, R. Kosloff, Quantum heat machines equivalence, work extraction beyond markovianity, and strong coupling via heat exchangers, Entropy 18 (4) (2016) http://dx.doi.org/10.3390/e18040124.
[17] M. Carrega, P. Solinas, M. Sassetti, U. Weiss, Energy exchange in driven open quantum systems at strong coupling, Phys. Rev. Lett. 116 (2016) 240403, http://dx.doi.org/10.1103/PhysRevLett.116.240403.
[18] C. Jarzynski, Stochastic and macroscopic thermodynamics of strongly coupled systems, Phys. Rev. X 7 (2017) 011008, http://dx.doi.org/10.1103/PhysRevX.7.011008.
[19] H.J.D. Miller, J. Anders, Entropy production and time asymmetry in the presence of strong interactions, Phys. Rev. E 95 (2017) 062123, http://dx.doi.org/10.1103/PhysRevE.95.062123.
[20] D. Newman, F. Mintert, A. Nazir, Performance of a quantum heat engine at strong reservoir coupling, Phys. Rev. E 95 (3) (2017) 032139, http://dx.doi.org/10.1103/PhysRevE.95.032139.
[21] E. Aurell, On work and heat in time-dependent strong coupling, Entropy 19 (11) (2017) http://dx.doi.org/10.3390/e19110595.
[22] W. Dou, M.A. Ochoa, A. Nitzan, J.E. Subotnik, Universal approach to quantum thermodynamics in the strong coupling regime, Phys. Rev. B 98 (13) (2018) 134306, http://dx.doi.org/10.1103/PhysRevB.98.134306.
[23] A. Bruch, C. Lewenkopf, F. von Oppen, Landauer-büttiker approach to strongly coupled quantum thermodynamics: Inside-outside duality of entropy evolution, PRL 120 (10) (2018) 107701, http://dx.doi.org/10.1103/PhysRevLett.120.107701.
[24] M. Perarnau-Llobet, H. Wilming, A. Riera, R. Gallego, J. Eisert, Strong coupling corrections in quantum thermodynamics, Phys. Rev. Lett. 120 (2018) 120602, http://dx.doi.org/10.1103/PhysRevLett.120.120602.
[25] Y.Y. Xu, J. Liu, M. Feng, Positive entropy production rate induced by non-markovianity, Phys. Rev. E 98 (3) (2018) 032102.
[26] K. Funo, H.T. Quan, Path integral approach to quantum thermodynamics, Phys. Rev. Lett. 121 (2018) 040602, http://dx.doi.org/10.1103/PhysRevLett.121.040602.
[27] P. Strasberg, M. Esposito, Non-markovianity and negative entropy production rates, Phys. Rev. E 99 (2019) 012120, http://dx.doi.org/10.1103/PhysRevE.99.012120.
[28] W.H. Zurek, Decoherence, einselection, and the quantum origins of the classical, Rev. Modern Phys. 75 (2003) 715–775, http://dx.doi.org/10.1103/RevModPhys.75.715.
[29] M. Schlosshauer, Decoherence and the Quantum-to-Classical Transition, Springer, 2007.
[30] C.K. Lee, J. Cao, J. Gong, Noncanonical statistics of a spin-boson model: Theory and exact monte carlo simulations, Phys. Rev. E 86 (2012) 021109, http://dx.doi.org/10.1103/PhysRevE.86.021109.
[31] J. Iles-Smith, N. Lambert, A. Nazir, Environmental dynamics, correlations, and the emergence of noncanonical equilibrium states in open quantum systems, Phys. Rev. A 90 (2014) 032114, http://dx.doi.org/10.1103/PhysRevA.90.032114.
[32] K. Goyal, R. Kawai, Steady state thermodynamics of two qubits strongly coupled to bosonic environments, arXiv:1712.09129.
[33] M. Campisi, P. Talkner, P. Hänggi, Fluctuation theorem for arbitrary open quantum systems, Phys. Rev. Lett. 102 (2009) 210401, http://dx.doi.org/10.1103/PhysRevLett.102.210401.
[34] A. Kato, Y. Tanimura, Quantum heat transport of a two-qubit system: Interplay between system-bath coherence and qubit-qubit coherence, J. Chem. Phys. 143 (6) (2015) 064107, http://dx.doi.org/10.1063/1.4928192.
[35] A. Kato, Y. Tanimura, Quantum heat current under non-perturbative and non-markovian conditions: Applications to heat machines, J. Chem. Phys. 145 (22) (2016) 224105, http://dx.doi.org/10.1063/1.4971370.
[36] C. Maier, T. Brydges, P. Jurcevic, N. Trautmann, C. Hempel, B.P. Lanyon, P. Hauke, R. Blatt, C.F. Roos, Environment-assisted quantum transport in a 10-qubit network, Phys. Rev. Lett. 122 (2019) 050501, http://dx.doi.org/10.1103/PhysRevLett.122.050501.
[37] T. Sagawa, M. Ueda, Second law of thermodynamics with discrete quantum feedback control, Phys. Rev. Lett. 100 (2008) 080403, http://dx.doi.org/10.1103/PhysRevLett.100.080403.
[38] T. Sagawa, M. Ueda, Minimal energy cost for thermodynamic information processing: measurement and information erasure, Phys. Rev. Lett. 102 (2009) 250602, http://dx.doi.org/10.1103/PhysRevLett.102.250602.
[39] S. Toyabe, T. Sagawa, M. Ueda, E. Muneyuki, M. Sano, Experimental demonstration of information-to-energy conversion and validation of the generalized jarzynski equality, Nat. Phys. 6 (2010) 988, http://dx.doi.org/10.1038/nphys1821.
[40] J.G. Kirkwood, Statistical mechanics of fluid mixtures, J. Chem. Phys. 3 (5) (1935) 300–313, http://dx.doi.org/10.1063/1.1749657.
[41] Y. Tanimura, Nonperturbative expansion method for a quantum system coupled to a harmonic-oscillator bath, Phys. Rev. A 41 (1990) 6676–6687.
[42] I. de Vega, D. Alonso, Dynamics of non-markovian open quantum systems, Rev. Mod. Phys. 89 (2017) 015001, http://dx.doi.org/10.1103/RevModPhys.89.015001.
[43] H.-P. Breuer, F. Petruccione, The Theory of Open Quantum Systems, Oxford University Press, 2002.
[44] E. Aurell, K. Goyal, R. Kawai, An operator derivation of the feynman-vernon theory, with applications to the generating function of bath energy changes and to anharmonic baths, arXiv:1907.02671.
[45] R.-X. Xu, B.-L. Tian, J. Xu, Q. Shi, Y. Yan, Hierarchical quantum master equation with semiclassical drude dissipation, J. Chem. Phys. 131 (21) (2009) 214111, http://dx.doi.org/10.1063/1.3268922.
[46] B.-L. Tian, J.-J. Ding, R.-X. Xu, Y. Yan, Biexponential theory of drude dissipation via hierarchical quantum master equation, J. Chem. Phys. 133 (11) (2010) 114112, http://dx.doi.org/10.1063/1.3491270.